

Lax-Wendroff and Nyström methods for seismic modelling

Jing-Bo Chen*

Key Laboratory of Integrative Researches on Geophysics for Petroleum Institute of Geology and Geophysics, Chinese Academy of Sciences
PO Box 9825, Beijing 100029, P.R. China

Received December 2007, revision accepted January 2009

ABSTRACT

Lax-Wendroff and Nyström methods are numerical algorithms of temporal approximations for solving differential equations. These methods provide efficient algorithms for high-accuracy seismic modeling. In the context of spatial pseudospectral discretizations, I explore these two kinds of methods in a comparative way. Their stability and dispersion relation are discussed in detail. Comparison between the fourth-order Lax-Wendroff method and a fourth-order Nyström method shows that the Nyström method has smaller stability limit but has a better dispersion relation, which is closer to the sixth-order Lax-Wendroff method. The structure-preserving property of these methods is also revealed. The Lax-Wendroff methods are a second-order symplectic algorithm, which is independent of the order of the methods. This result is useful for understanding the error growth of Lax-Wendroff methods. Numerical experiments based on the scalar wave equation are performed to test the presented schemes and demonstrate the advantages of the symplectic methods over the nonsymplectic ones.

INTRODUCTION

Seismic modelling plays an important role in exploration seismology. Synthetic seismograms produced through seismic modelling provide valuable information in seismic interpretation and exploration. Seismic modelling methods can be classified into three main categories: direct methods, integral-equation methods, and ray-tracing methods (Carcione, Herman and ten Kroode 2002).

High-accuracy seismic modelling schemes become increasingly important due to practical needs for accurate seismic interpretation and exploration. Numerical schemes for direct methods of seismic modelling involve discretization of both space and time variables. Spatial discretizations have been extensively explored and three approaches have been developed: finite-difference methods (Alford, Kelly and Boore 1974; Kelly *et al.* 1976; Virieux 1986), pseudospectral methods (Gazdag 1981; Kosloff and Baysal 1982; Kosloff, Reshef and

Loewental 1984; Fornberg 1987) and finite-element methods (Marfurt 1984). Some combinations of these methods are also available, such as spectral-element methods (Komatitsch and Vilotte 1998) and finite-volume methods (Dormy and Tarantola 1995). In terms of accuracy, pseudospectral methods and related spectral-element methods are appropriate candidates. In this paper, I will use pseudospectral spatial discretizations.

On the other hand, methods for time discretizations have been relatively less studied. Second-order finite-difference discretizations have been widely used. Lax-Wendroff methods produce high-order time discretizations by using spatial derivatives to replace high-order temporal derivatives (Dablain 1986; Carcione *et al.* 2002). Nyström methods are numerical methods designed for second-order differential equations and they are simplified Runge-Kutta methods (Hairer, Nsett and Warnner 1993). Nyström methods for modeling the scalar wave equation were discussed in Chen (2006). An accurate time discretization based on Chebyshev polynomials was presented by Tal-Ezer, Kosloff and Koren (1987).

*E-mail: chenjb@vip.sohu.com

Recently, high-order time discretizations were examined in Chen (2007). In this paper, I will further develop the results in Chen (2007). The main advances include: 1) A detailed analysis of stability and dispersion relations for both Lax-Wendroff and Nyström methods are given, and comparison between them is discussed; 2) the structure-preserving property of the Lax-Wendroff methods is revealed and this result lends itself to understanding the error growth of the methods.

In the next section, the pseudospectral methods are presented briefly. I then discuss the structure-preserving property of numerical methods. This is followed by a presentation of Lax-Wendroff and Nyström methods. After this, I explore in detail the dispersion relation and stability for these two kinds of methods and make comparisons between them. Finally, numerical experiments are performed to illustrate the presented schemes.

PSEUDOSPECTRAL SPATIAL DISCRETIZATIONS

In this section, I will briefly present the pseudospectral methods for the scalar wave equation.

Consider the scalar wave equation

$$\frac{\partial^2 u}{\partial t^2} = c^2 \left(\frac{\partial^2 u}{\partial x^2} + \frac{\partial^2 u}{\partial y^2} + \frac{\partial^2 u}{\partial z^2} \right), \tag{1}$$

where $u(x, y, z, t)$ is the wavefield and $c(x, y, z)$ is the velocity. Let $\mathbf{u} = [u_{1,1,1}, \dots, u_{N_x, N_y, N_z}]^T$, where T represents transpose and $u_{i,j,l}$ are the wavefield values at discrete locations, i.e., $u_{i,j,l} \approx u(i\Delta x, j\Delta y, l\Delta z, t)$, $i = 1, \dots, N_x$; $j = 1, \dots, N_y$; $l = 1, \dots, N_z$. $\Delta x, \Delta y$ and Δz are grid spacings in the x, y and z directions and N_x, N_y and N_z are sampling numbers in the x, y and z directions, respectively. Here, for simplicity, we consider a computational domain $[0, X] \times [0, Y] \times [0, Z]$. Therefore, $\Delta x = \frac{X}{N_x}$, $\Delta y = \frac{Y}{N_y}$, and $\Delta z = \frac{Z}{N_z}$. The semi-discrete system resulting from the pseudospectral method for equation (1) is

$$\frac{d^2 \mathbf{u}}{dt^2} = c^2 \mathcal{F}^{-1} [\mathbf{k}^2 * \mathcal{F}(\mathbf{u})], \tag{2}$$

where \mathcal{F} and \mathcal{F}^{-1} represent three-dimensional forward and inverse finite Fourier transforms respectively, $\mathbf{k}^2 = [k_{1,1,1}^2, \dots, k_{N_x, N_y, N_z}^2]^T$ with $k_{i,j,l}^2 = -(k_{x_i}^2 + k_{y_j}^2 + k_{z_l}^2)$, where k_{x_i}, k_{y_j} and k_{z_l} are discrete wavenumbers in the x, y and z directions, respectively. The star $*$ denotes array multiplication between vectors. For example, suppose that we have two vectors $\mathbf{s} = (s_1, s_2, \dots, s_m)$ and $\mathbf{t} = (t_1, t_2, \dots, t_m)$, then $\mathbf{s} * \mathbf{t} = (s_1 t_1, s_2 t_2, \dots, s_m t_m)$.

A good and comprehensive introduction of the pseudospectral method was given in the context of seismic modelling by Fornberg (1987). There, the pseudospectral method was presented in terms of both a limit of finite-difference of increasing orders and trigonometric interpolation. In particular, the pseudospectral methods for step functions and for variable coefficients were examined. In the step-function case, due to Gibb's phenomenon, the pseudospectral method is not appropriate to compute the derivative at a fixed time. However, in seismic modelling, we solve the wave equation numerically over a long time and the oscillatory errors cancel to produce a high accuracy. The same argument applies to the variable-coefficient case. For media with interfaces, the pseudospectral method has large local errors due to Gibb's phenomenon at a discontinuity but the global errors grow very little with time because of cancellations. For details and related numerical tests, see Fornberg (1987).

STRUCTURE-PRESERVING PROPERTY OF NUMERICAL METHODS

Continuous differential equations usually possess various structures such as symplectic structure (Hairer, Lubich and Warnner 2002). When solving these continuous differential equations numerically, some numerical schemes also preserve the corresponding structures. This is called the structure-preserving property of a numerical scheme.

In this paper, we are only concerned with the so-called symplectic structure and symplectic algorithms. We now briefly discuss the symplectic structure and symplectic algorithms for Hamiltonian systems. For details, see Sanz-Serna and Calvo (1994) and Hairer *et al.* (2002).

A Hamiltonian system is a system of ordinary equations with the following form

$$\begin{aligned} \frac{d\mathbf{p}}{dt} &= -\frac{\partial H(\mathbf{p}, \mathbf{q})}{\partial \mathbf{q}}, \\ \frac{d\mathbf{q}}{dt} &= \frac{\partial H(\mathbf{p}, \mathbf{q})}{\partial \mathbf{p}}, \end{aligned} \tag{3}$$

where $\mathbf{p} = (p_1, p_2, \dots, p_n)$ is the generalized coordinate, $\mathbf{q} = (q_1, q_2, \dots, q_n)$ is the generalized momentum and $H(\mathbf{p}, \mathbf{q})$ is the Hamiltonian function.

Suppose that the solution of the Hamiltonian system (3) is $Z = F(Z_0)$, where $Z = [\mathbf{p}(t), \mathbf{q}(t)]^T$ and $Z_0 = [\mathbf{p}(0), \mathbf{q}(0)]^T$. The solution $Z = F(Z_0)$ satisfies

$$\left[\frac{\partial F}{\partial Z_0} \right] J \left[\frac{\partial F}{\partial Z_0} \right]^T = J, \quad \text{where } J = \begin{bmatrix} 0 & I \\ -I & 0 \end{bmatrix}. \tag{4}$$

Here $\left[\frac{\partial F}{\partial Z_0}\right]$ is the Jacobian of the vector-valued function $F(Z_0)$ and I the $n \times n$ identity matrix. A function satisfying the above equality is called a symplectic mapping. Therefore, the true solution of a Hamiltonian system is a symplectic mapping. A numerical method for Hamiltonian systems is called a symplectic algorithm if the resulting numerical solution is also a symplectic mapping. The numerical solution obtained by a symplectic algorithm exactly satisfies a perturbed Hamiltonian system. This property guarantees that symplectic algorithms have slower error growth and possess remarkable capability in preserving conservative quantities. Therefore, symplectic algorithms play an important role in high-accuracy or long-time numerical simulations.

LAX-WENDROFF AND NYSTRÖM METHODS

Lax-Wendroff methods

Based on Taylor expansions, Lax-Wendroff methods use spatial derivatives to replace high-order temporal derivatives (Dablain 1986; Carcione *et al.* 2002):

$$\frac{u^{n+1} - 2u^n + u^{n-1}}{\Delta t^2} = c^2 \left(\frac{\partial^2 u^n}{\partial x^2} + \frac{\partial^2 u^n}{\partial y^2} + \frac{\partial^2 u^n}{\partial z^2} \right) + 2 \sum_{j=2}^J \frac{(\Delta t)^{2j-2}}{(2j)!} \frac{\partial^{2j} u^n}{\partial t^{2j}}, \quad (5)$$

where $u^n \approx u(x, y, z, n\Delta t)$, Δt is the time-step size and the temporal derivatives are obtained by the following recursive formula:

$$\begin{aligned} \frac{\partial^2 u^n}{\partial t^2} &= c^2 \left(\frac{\partial^2 u^n}{\partial x^2} + \frac{\partial^2 u^n}{\partial y^2} + \frac{\partial^2 u^n}{\partial z^2} \right), \\ \frac{\partial^{2j} u^n}{\partial t^{2j}} &= c^2 \left(\frac{\partial^2}{\partial x^2} + \frac{\partial^2}{\partial y^2} + \frac{\partial^2}{\partial z^2} \right) \frac{\partial^{2j-2} u^n}{\partial t^{2j-2}}, \quad j = 2, 4, \dots, J. \end{aligned}$$

Scheme (5) has accuracy of $\mathcal{O}((\Delta t)^{2J})$. Using pseudospectral spatial discretization, scheme (5) becomes

$$\frac{u^{n+1} - 2u^n + u^{n-1}}{\Delta t^2} = c^2 \mathcal{F}^{-1} [k^2 * \mathcal{F}(u^n)] + 2 \sum_{j=2}^J \frac{(\Delta t)^{2j-2}}{(2j)!} \frac{\partial^{2j} u^n}{\partial t^{2j}}, \quad (6)$$

where

$$\begin{aligned} \frac{\partial^2 u^n}{\partial t^2} &= c^2 \mathcal{F}^{-1} [k^2 * \mathcal{F}(u^n)] \\ \frac{\partial^{2j} u^n}{\partial t^{2j}} &= c^2 \mathcal{F}^{-1} \left[k^2 * \mathcal{F} \left(\frac{\partial^{2j-2} u^n}{\partial t^{2j-2}} \right) \right], \quad j = 2, 4, \dots, J. \end{aligned}$$

Since we use pseudospectral spatial discretization, the spatial accuracy is of exponential order $\mathcal{O}(\exp(\Delta x, \Delta y, \Delta z))$

(Fornberg 1996). Therefore, the accuracy of scheme (6) is $\mathcal{O}((\Delta t)^{2J} + \exp(\Delta x, \Delta y, \Delta z))$.

The starting value u^n in scheme (6) can be obtained through the following Taylor expansion

$$u(n\Delta t) = \sum_{i=0}^{2J} \frac{\partial^i u((n-1)\Delta t)}{\partial t^i} \frac{(\Delta t)^i}{i!},$$

where the temporal derivatives are obtained in the same way as in scheme (5).

We now consider the structure-preserving property of the scheme (6). Introducing a new variable $v = \frac{du}{dt}$, the scheme (6) is equivalent to the following scheme

$$\begin{aligned} v^{n+\frac{1}{2}} &= v^n + \frac{\Delta t}{2} G(u^n), \\ u^{n+1} &= u^n + \Delta t v^{n+\frac{1}{2}}, \\ v^{n+1} &= v^{n+\frac{1}{2}} + \frac{\Delta t}{2} G(u^{n+1}), \end{aligned} \quad (7)$$

where

$$G(u^n) = c^2 \mathcal{F}^{-1} [k^2 * \mathcal{F}(u^n)] + 2 \sum_{j=2}^J \frac{(\Delta t)^{2j-2}}{(2j)!} \frac{\partial^{2j} u^n}{\partial t^{2j}}.$$

Scheme (7) is called the Störmer-Verlet method. The Störmer-Verlet method is a symplectic algorithm with accuracy of $\mathcal{O}(\Delta t^2)$. For details, see (Hairer *et al.* 2002).

Although the structure-preserving property of the Störmer-Verlet method is well-known, the structure-preserving property of the Lax-Wendroff scheme (6) has its unique and interesting point. The accuracy of time discretization in scheme (6) is $\mathcal{O}((\Delta t)^{2J})$, however, as a symplectic algorithm, scheme (6) has an accuracy of $\mathcal{O}((\Delta t)^2)$ which is independent of the values of J . This is because the high-order time discretization in scheme (6) is reached through spatial discretizations while the structure-preserving property of scheme (6) is based on a second-order time discretization. In fact, scheme (7) can be regarded as a second-order time discretization of the following equation

$$\frac{\partial^2 u^n}{\partial t^2} = c^2 \left(\frac{\partial^2 u^n}{\partial x^2} + \frac{\partial^2 u^n}{\partial y^2} + \frac{\partial^2 u^n}{\partial z^2} \right) + 2 \sum_{j=2}^J \frac{(\Delta t)^{2j-2}}{(2j)!} \frac{\partial^{2j} u^n}{\partial t^{2j}}, \quad (8)$$

where the temporal derivatives are obtained in the same way as in equation (5). Equation (8) can be viewed as a modified version of the equation (1). It should be noted that although scheme (7) has accuracy of $\mathcal{O}((\Delta t)^2)$ with respect to equation (8), it still has accuracy of $\mathcal{O}((\Delta t)^{2J})$ with respect to equation (1).

Nyström methods

Nyström methods are numerical methods designed for second-order differential equations. Nyström (1925) first considered this as a simplification of Runge-Kutta methods. Nyström methods were systematically developed by Hairer *et al.* (1993).

To construct a Nyström method, we first introduce new variables and recast the second-order equation under consideration into a system of first-order equations. Then we apply Runge-Kutta methods to the system of first-order equations and take advantage of the special form of the equation to make simplifications.

For our purposes, consider a second-order system of ordinary differential equations written in the form

$$\frac{d^2 \mathbf{y}}{dt^2} = \mathbf{f}(t, \mathbf{y}). \tag{9}$$

Introducing $\mathbf{z} = d \mathbf{y}/dt$, we can recast equation (9) as

$$\begin{aligned} \frac{d \mathbf{y}}{dt} &= \mathbf{z}, \\ \frac{d \mathbf{z}}{dt} &= \mathbf{f}(t, \mathbf{y}). \end{aligned} \tag{10}$$

A Nyström method for system (10) reads

$$\begin{aligned} \mathbf{Z}_i &= \mathbf{f}(n\Delta t + c_i \Delta t, \mathbf{y}^n + c_i \Delta t \mathbf{z}^n + \Delta t^2 \sum_{j=1}^s a_{ij} \mathbf{Z}_j), \\ &\quad i = 1, 2, \dots, s, \\ \mathbf{y}^{n+1} &= \mathbf{y}^n + \Delta t \mathbf{z}^n + \Delta t^2 \sum_{i=1}^s \bar{b}_i \mathbf{Z}_i, \\ \mathbf{z}^{n+1} &= \mathbf{z}^n + \Delta t \sum_{i=1}^s b_i \mathbf{Z}_i, \end{aligned} \tag{11}$$

where $\mathbf{y}^n = \mathbf{y}(n\Delta t)$, $\mathbf{z}^n = \mathbf{z}(n\Delta t)$, $\mathbf{y}^{n+1} \approx \mathbf{y}((n+1)\Delta t)$, $\mathbf{z}^{n+1} \approx \mathbf{z}((n+1)\Delta t)$, Δt is the time step size and c_i , a_{ij} , \bar{b}_i and b_i are constants that determine the order of the method.

We now suppose that the system (10) is a Hamiltonian system. Namely, we can reformulate (10) as

$$\frac{d}{dt} \begin{bmatrix} \mathbf{y} \\ \mathbf{z} \end{bmatrix} = \begin{bmatrix} 0 & I \\ -I & 0 \end{bmatrix} \begin{bmatrix} \frac{\partial H}{\partial \mathbf{y}} \\ \frac{\partial H}{\partial \mathbf{z}} \end{bmatrix}, \tag{12}$$

where I is an identity matrix, $H = \frac{1}{2}[\mathbf{z}^T \mathbf{z} - \mathbf{y}^T D \mathbf{y}]$ and D is a matrix satisfying $D \mathbf{y} = \mathbf{f}(t, \mathbf{y})$.

In this case, if the coefficients in scheme (11) satisfy

$$\begin{aligned} \bar{b}_i &= b_i(1 - c_i), \quad i = 1, \dots, s, \\ b_i(\bar{b}_j - a_{ij}) &= b_j(\bar{b}_i - a_{ji}), \quad i, j = 1, \dots, s, \end{aligned}$$

then scheme (11) is a symplectic Nyström algorithm (Sanz-serna and Calvo 1994).

In this paper, we consider a fourth-order explicit symplectic method (Qin and Zhu 1991) for the semi-discrete wave equation (2):

$$\begin{aligned} \mathbf{V}_1 &= c^2 \mathcal{F}^{-1}[\mathbf{w} * \mathcal{F}(\mathbf{u}^n + d_1 \Delta t \mathbf{v}^n)], \\ \mathbf{V}_2 &= c^2 \mathcal{F}^{-1}[\mathbf{w} * \mathcal{F}(\mathbf{u}^n + d_2 \Delta t \mathbf{v}^n + a_{21}(\Delta t)^2 \mathbf{V}_1)], \\ \mathbf{V}_3 &= c^2 \mathcal{F}^{-1}[\mathbf{w} * \mathcal{F}(\mathbf{u}^n + d_3 \Delta t \mathbf{v}^n + a_{31}(\Delta t)^2 \mathbf{V}_1 \\ &\quad + a_{32}(\Delta t)^2 \mathbf{V}_2)], \\ \mathbf{u}^{n+1} &= \mathbf{u}^n + \Delta t \mathbf{v}^n + (\Delta t)^2 (\bar{b}_1 \mathbf{V}_1 + \bar{b}_2 \mathbf{V}_2 + \bar{b}_3 \mathbf{V}_3), \\ \mathbf{v}^{n+1} &= \mathbf{v}^n + \Delta t (b_1 \mathbf{V}_1 + b_2 \mathbf{V}_2 + b_3 \mathbf{V}_3), \end{aligned} \tag{13}$$

where

$$\begin{aligned} d_1 &= \frac{3 + \sqrt{3}}{6}, \quad d_2 = \frac{3 - \sqrt{3}}{6}, \quad d_3 = \frac{3 + \sqrt{3}}{6}, \quad \bar{b}_1 = \frac{5 - 3\sqrt{3}}{24}, \\ \bar{b}_2 &= \frac{3 + \sqrt{3}}{12}, \quad \bar{b}_3 = \frac{1 + \sqrt{3}}{24}, \quad b_1 = \frac{3 - 2\sqrt{3}}{12}, \quad b_2 = \frac{1}{2}, \\ b_3 &= \frac{3 + 2\sqrt{3}}{12}, \\ a_{21} &= \frac{2 - \sqrt{3}}{12}, \quad a_{31} = 0, \quad a_{32} = \frac{\sqrt{3}}{6}. \end{aligned}$$

The accuracy of equation (3) is $\mathcal{O}(\Delta t^4 + \exp(\Delta x, \Delta y, \Delta z))$.

Okunbor and Skeel (1992) presented explicit symplectic Nyström algorithms of orders 5 and 6. A seventh-order explicit symplectic Nyström algorithm was obtained by Calvo and Sanz-Serna (1993). Tsitouras (1999) developed a tenth-order explicit symplectic Nyström algorithm. Some optimized symplectic Nyström algorithms have also been developed (Blanes and Moan 2002; Lunk and Simen 2005).

DISPERSION RELATION AND STABILITY

We now perform analysis of dispersion relation and stability for the Lax-Wendroff scheme (6) and the Nyström scheme (13).

Lax-Wendroff scheme (equation (6))

Dispersion relation. We substitute the expression $\exp\{i(\omega t - k_x x - k_y y - k_z z)\}$ into equation (6) and obtain the dispersion relation

$$\sin^2 \frac{\omega \Delta t}{2} = \frac{1}{4} \left\{ (ck\Delta t)^2 - 2 \sum_{j=2}^J (-1)^j \frac{(ck\Delta t)^{2j}}{(2j)!} \right\}, \tag{14}$$

where $k = \sqrt{k_x^2 + k_y^2 + k_z^2}$.

For $J = 2$, equation (14) becomes

$$\sin^2 \frac{\omega \Delta t}{2} = \frac{1}{4} \left\{ (ck\Delta t)^2 - \frac{1}{12} (ck\Delta t)^4 \right\}. \quad (15)$$

For $J = 3$, equation (14) becomes

$$\sin^2 \frac{\omega \Delta t}{2} = \frac{1}{4} \left\{ (ck\Delta t)^2 - \frac{1}{12} (ck\Delta t)^4 + \frac{1}{360} (ck\Delta t)^6 \right\}. \quad (16)$$

Let \bar{c} denote the phase velocity determined by equation (14). From dispersion relation (14), we can derive the normalized phase velocity

$$\frac{\bar{c}}{c} = \frac{2}{rk\Delta x} \sin^{-1} \left\{ \frac{rk\Delta x}{2} \sqrt{1 - 2 \sum_{j=2}^J (-1)^j \frac{(rk\Delta x)^{2j-2}}{(2j)!}} \right\}, \quad (17)$$

where $r = \frac{c\Delta t}{\Delta x}$ is the Courant number.

In the upper plot of Fig. 1, I show the normalized phase velocity (17) with $J = 2$ for different r values. We find that the normalized phase velocity is approximately accurate for all wavenumbers for $r = 0.3$. For larger r values, the dispersion curves deviate from the exact curve for large wavenumbers.

I show the dispersion curves for different J values in the lower plot of Fig. 1. In this case, I take a fixed Courant number ($r = 0.5$). We can see that the normalized phase velocity is approximately accurate for all wavenumbers for $J = 4$ or larger. From the stability analysis below, we can see that the r value 0.5 is near the stability limits of scheme (6) for $J \geq 4$. This means that, for $J \geq 4$, we can use the Courant number in the vicinity of stability limits while at the same time achieving an approximately accurate dispersion relation.

Stability. The stability limit of scheme (6) can be obtained by solving the following inequality

$$0 \leq \frac{1}{4} \left\{ c^2 k^2 \Delta t^2 - 2 \sum_{j=2}^J (-1)^j \frac{(ck\Delta t)^{2j}}{(2j)!} \right\} \leq 1. \quad (18)$$

With $J = 2$, inequality (18) becomes

$$0 \leq (ck\Delta t)^2 - \frac{1}{12} (ck\Delta t)^4 \leq 4. \quad (19)$$

From equation (19), we obtain $ck\Delta t \leq \sqrt{12}$. For a uniform spacing $\Delta x = \Delta y = \Delta z = h$, we have the Nyquist frequencies $k_x = k_y = k_z = \frac{\pi}{h}$. In this case, the stability limit of equation (6) with $J = 2$ becomes

$$r = \frac{c\Delta t}{h} \leq \frac{2}{\pi}. \quad (20)$$

With $J = 3$, inequality (18) becomes

$$0 \leq (ck\Delta t)^2 - \frac{1}{12} (ck\Delta t)^4 + \frac{1}{360} (ck\Delta t)^6 \leq 4. \quad (21)$$

Solving equation (21), we can obtain the stability limit of equation (6) with $J = 3$:

$$r = \frac{c\Delta t}{h} \leq \frac{\sqrt{10 + 2\sqrt[3]{5} - 2\sqrt[3]{25}}}{\sqrt{3}\pi} \approx \frac{1.5887}{\pi}. \quad (22)$$

For $J = 4$, we can also obtain the analytic expression for the stability limit that is very tedious and complicated. For $J \geq 5$, analytical expressions for the stability limits are not available in general and we can only obtain the approximate stability limit by numerically solving equation (18). In Table 1, I list the stability limits of scheme (6) up to $J = 8$. For completeness, the stability limits for one- and two-dimensional cases are also listed. We find that stability limits increase and decrease alternately. This is because the terms in equation (18) change signs (plus and minus) alternately. When a plus term is added, the value of the stability limit decreases a bit and when a minus term is added, the value of the stability limit increases a bit. However, since the coefficients of added terms decrease rapidly with increasing J , the amplitude of the change in the stability limits also decrease rapidly. Actually, we can use the stability limit $\frac{1.5963}{\pi}$ for $J \geq 7$ (three-dimensional case) in practice.

Fourth-order Nyström scheme (equation 13)

Stability. We first make simple variable transform $\tilde{\mathbf{v}} = \mathbf{v}\Delta t$ in order to obtain polynomials in $ck\Delta t$. Let $A = [A_1, A_2]^T$ be a constant vector. We substitute the expression

$$\begin{bmatrix} \mathbf{u} \\ \tilde{\mathbf{v}} \end{bmatrix} = \begin{bmatrix} A_1 \\ A_2 \end{bmatrix} \exp\{i(\omega t - k_x x - k_y y - k_z z)\}$$

into equation (13) and obtain

$$\exp(i\omega\Delta t) \begin{bmatrix} A_1 \\ A_2 \end{bmatrix} = \begin{bmatrix} 1 - \frac{1}{2}\theta^2 + \frac{1}{24}\theta^4 - \frac{3-\sqrt{3}}{1728}\theta^6 & 1 - \frac{1}{6}\theta^2 + \frac{1}{72}\theta^4 - \frac{1}{1728}\theta^6 \\ -\theta^2 + \frac{1}{6}\theta^4 - \frac{1}{288}\theta^6 & 1 - \frac{1}{2}\theta^2 + \frac{1}{24}\theta^4 - \frac{3+\sqrt{3}}{1728}\theta^6 \end{bmatrix} \times \begin{bmatrix} A_1 \\ A_2 \end{bmatrix}, \quad (23)$$

where $\theta = ck\Delta t$.

Equation (23) forms an eigenvalue problem. The eigenvalues are

$$\lambda = \left(1 - \frac{1}{2}\theta^2 + \frac{1}{24}\theta^4 - \frac{1}{576}\theta^6 \right) \pm \sqrt{\left(1 - \frac{1}{2}\theta^2 + \frac{1}{24}\theta^4 - \frac{1}{576}\theta^6 \right)^2 - 1}. \quad (24)$$

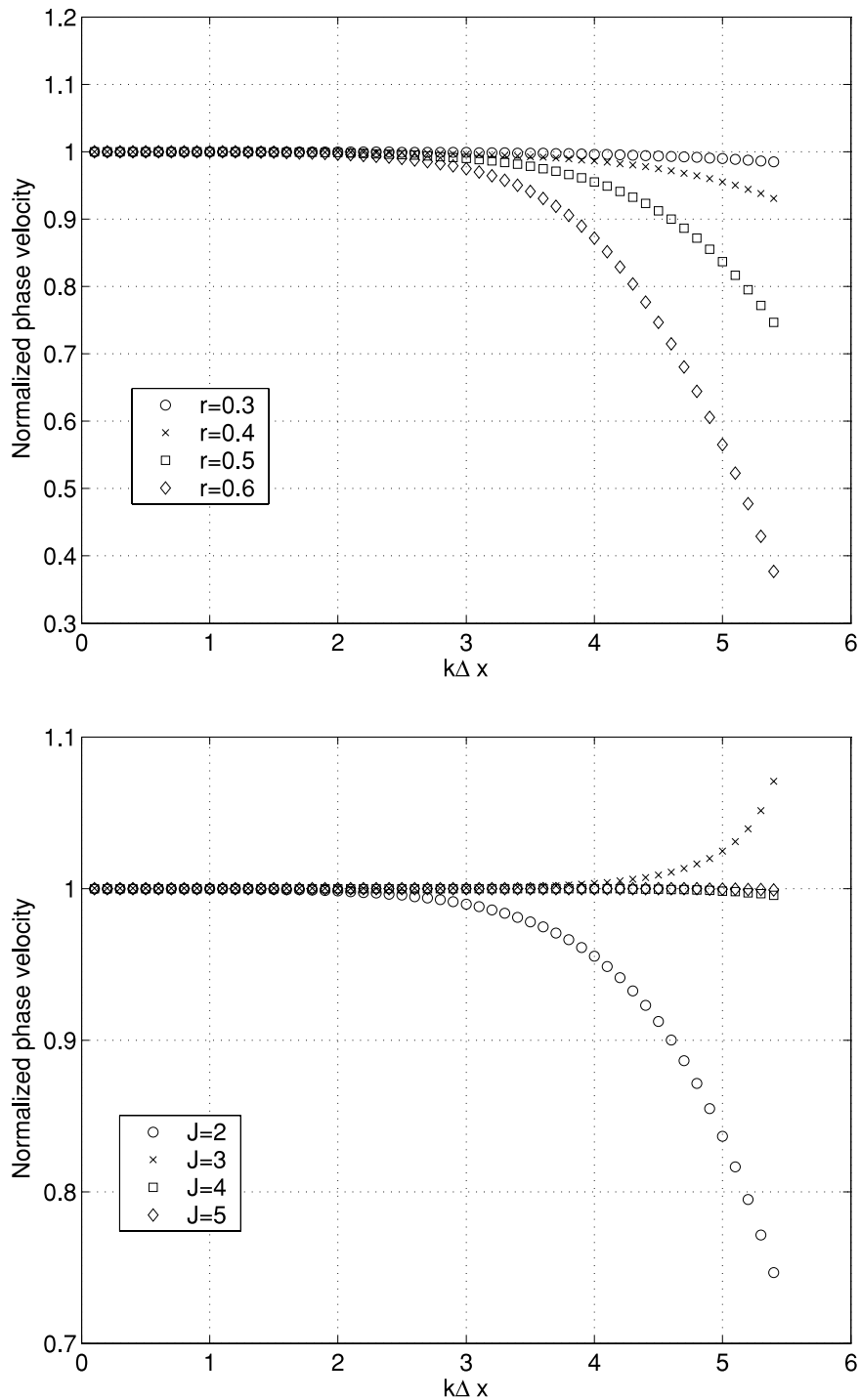


Figure 1 Upper plot: normalized phase velocity of scheme (6) versus wavenumbers for different Courant numbers. Lower plot: normalized phase velocity of scheme (6) versus wavenumbers for different J with $r = 0.5$.

To insure that $|\lambda| = 1$, we have

$$\left| 1 - \frac{1}{2}\theta^2 + \frac{1}{24}\theta^4 - \frac{1}{576}\theta^6 \right| \leq 1. \quad (25)$$

From equation (25), we obtain the stability limit

$$\theta \leq 2\sqrt{2 + \sqrt[3]{2} - \sqrt[3]{4}}. \quad (26)$$

Table 1 Stability limits of scheme (6)

	$J = 2$	$J = 3$	$J = 4$	$J = 5$	$J = 6$	$J = 7$	$J = 8$
1D	$\frac{2\sqrt{3}}{\pi}$	$\frac{2.7517115}{\pi}$	$\frac{2.7661347}{\pi}$	$\frac{2.7648554}{\pi}$	$\frac{2.7649292}{\pi}$	$\frac{2.7649286}{\pi}$	$\frac{2.7649286}{\pi}$
2D	$\frac{\sqrt{6}}{\pi}$	$\frac{1.9457539}{\pi}$	$\frac{1.9559526}{\pi}$	$\frac{1.9550480}{\pi}$	$\frac{1.9551002}{\pi}$	$\frac{1.95509980}{\pi}$	$\frac{1.95509980}{\pi}$
3D	$\frac{2}{\pi}$	$\frac{1.5887014}{\pi}$	$\frac{1.5970286}{\pi}$	$\frac{1.5962900}{\pi}$	$\frac{1.5963326}{\pi}$	$\frac{1.5963323}{\pi}$	$\frac{1.5963323}{\pi}$

Table 2 Stability limits of scheme (13)

1D	2D	3D
$\frac{2\sqrt{2+\sqrt[3]{2}-\sqrt[3]{4}}}{\pi} \approx \frac{2.5865}{\pi}$	$\frac{2\sqrt{2+\sqrt[3]{2}-\sqrt[3]{4}}}{\sqrt{2}\pi} \approx \frac{1.8289}{\pi}$	$\frac{2\sqrt{2+\sqrt[3]{2}-\sqrt[3]{4}}}{\sqrt{3}\pi} \approx \frac{1.4933}{\pi}$

For a uniform spacing $\Delta x = \Delta y = \Delta z = h$, the stability limit of equation (26) becomes

$$r = \frac{c\Delta t}{h} \leq \frac{2\sqrt{2+\sqrt[3]{2}-\sqrt[3]{4}}}{\sqrt{3}\pi} \approx \frac{1.4933}{\pi}. \tag{27}$$

In Table 2, I list the stability limits of scheme (13) for one-, two- and three-dimensional cases.

Dispersion relation. From equations (23) and (24), we can obtain the dispersion relation of the scheme (13):

$$\cos(\omega\Delta t) = 1 - \frac{1}{2}(ck\Delta t)^2 + \frac{1}{24}(ck\Delta t)^4 - \frac{1}{576}(ck\Delta t)^6. \tag{28}$$

Equation (28) can be simplified as

$$\sin^2 \frac{\omega\Delta t}{2} = \frac{1}{4} \left\{ (ck\Delta t)^2 - \frac{1}{12}(ck\Delta t)^4 + \frac{1}{288}(ck\Delta t)^6 \right\}. \tag{29}$$

Let \bar{c} denote the phase velocity determined by equation (29). From the dispersion relation (29), we can derive the normalized phase velocity

$$\frac{\bar{c}}{c} = \frac{2}{rk\Delta x} \sin^{-1} \left\{ \frac{rk\Delta x}{2} \sqrt{1 - \frac{1}{12}(rk\Delta x)^2 + \frac{1}{288}(rk\Delta x)^4} \right\}. \tag{30}$$

Now we make comparisons on dispersion relation and stability between Lax-Wendroff scheme (6) and Nyström scheme (13). In Fig. 2, I show the normalized phase velocity curves for Nyström scheme (13), fourth-order Lax-Wendroff scheme and sixth-order Lax-Wendroff scheme, respectively. We can see that the normalized phase velocity for equation (13) is better than that of the fourth-order Lax-Wendroff scheme and it is closer to that of the sixth-order Lax-Wendroff scheme. However, in terms of stability limit, the fourth-order Lax-Wendroff scheme is better than scheme (13). Actually, scheme

(13) behaves more like the sixth-order Lax-Wendroff scheme because the stability limit of the sixth-order Lax-Wendroff scheme is not as good as the fourth-order Lax-Wendroff scheme either. These observations can be explained by the dispersion relations (15), (16) and (29).

NUMERICAL EXPERIMENTS

In this section, we perform numerical experiments to test the Lax-Wendroff scheme (6) ($J = 2$) and the Nyström scheme (13), and make some numerical comparisons. Taking $J = 2$ in scheme (6), we obtain

$$\frac{\mathbf{u}^{n+1} - 2\mathbf{u}^n + \mathbf{u}^{n-1}}{\Delta t^2} = c^2 \mathcal{F}^{-1} \left[\mathbf{k}^2 * \mathcal{F}(\mathbf{u}^n) \right] + \frac{c^2(\Delta t)^2}{12} \mathcal{F}^{-1} \left\{ \mathbf{k}^2 * \mathcal{F} \left[c^2 \mathcal{F}^{-1} (\mathbf{k}^2 * \mathcal{F}(\mathbf{u}^n)) \right] \right\}. \tag{31}$$

To make comparisons, we also consider one scheme (Chen 2006):

$$\begin{aligned} \mathbf{V}_1 &= c^2 \mathcal{F}^{-1} [\mathbf{k}^2 * \mathcal{F}(\mathbf{u}^n)], \\ \mathbf{V}_2 &= c^2 \mathcal{F}^{-1} \left[\mathbf{k}^2 * \mathcal{F} \left(\mathbf{u}^n + \frac{1}{2} \Delta t \mathbf{v}^n + \frac{1}{8} \Delta t^2 \mathbf{V}_1 \right) \right], \\ \mathbf{V}_3 &= c^2 \mathcal{F}^{-1} \left[\mathbf{k}^2 * \mathcal{F} \left(\mathbf{u}^n + \Delta t \mathbf{v}^n + \frac{1}{2} \Delta t^2 \mathbf{V}_2 \right) \right], \\ \mathbf{u}^{n+1} &= \mathbf{u}^n + \Delta t \mathbf{v}^n + \Delta t^2 \left(\frac{1}{6} \mathbf{V}_1 + \frac{1}{3} \mathbf{V}_2 \right), \\ \mathbf{v}^{n+1} &= \mathbf{v}^n + \Delta t \left(\frac{1}{6} \mathbf{V}_1 + \frac{2}{3} \mathbf{V}_2 + \frac{1}{6} \mathbf{V}_3 \right). \end{aligned} \tag{32}$$

Schemes (31), (13) and (32) both have fourth-order accuracy in temporal discretizations. However, scheme (31) is a second-order symplectic algorithm, scheme (13) is a fourth-order symplectic algorithm and scheme (32) is a nonsymplectic algorithm. Therefore, these algorithms have different error growth. We will demonstrate this point in the following experiments. Since we focus on the temporal discretizations, we consider the two-dimensional case for clarity and simplicity. As in Gazdag (1981), we use the initial conditions

$$u(x, z, t = 0) = \exp[-0.0001(x^2 + (z - z_0)^2)], \quad \frac{\partial u(0)}{\partial t} = 0.$$

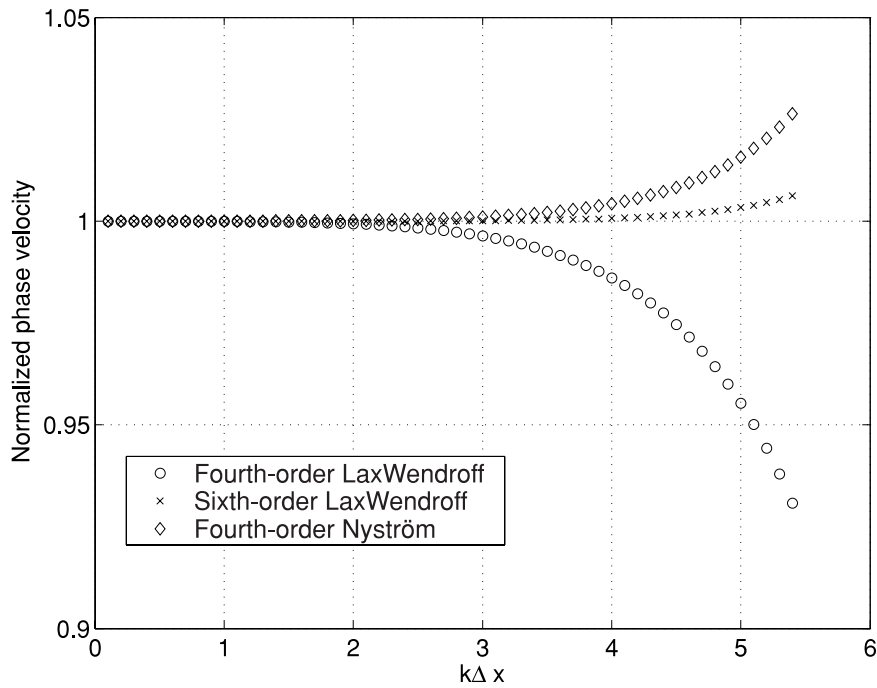


Figure 2 Normalized phase velocity of scheme (13), fourth-order Lax-Wendroff scheme and sixth-order Lax-Wendroff scheme. We take $r = 0.4$.

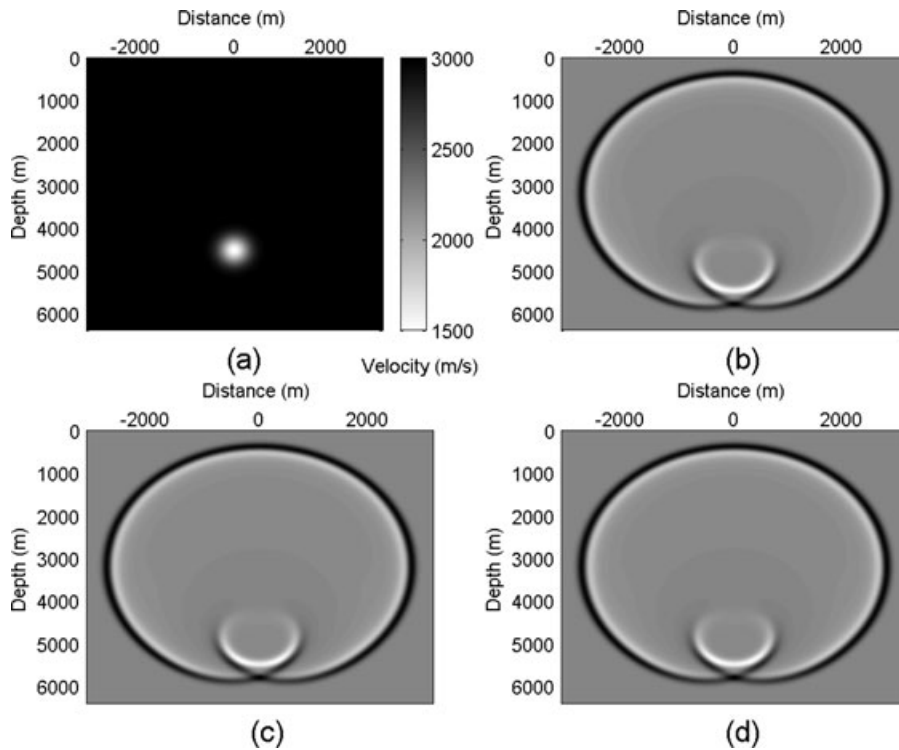


Figure 3 The velocity model (plot a) and wavefields at time $t = 0.92$ s computed with schemes (31) (plot b), (13) (plot c) and (32) (plot d).

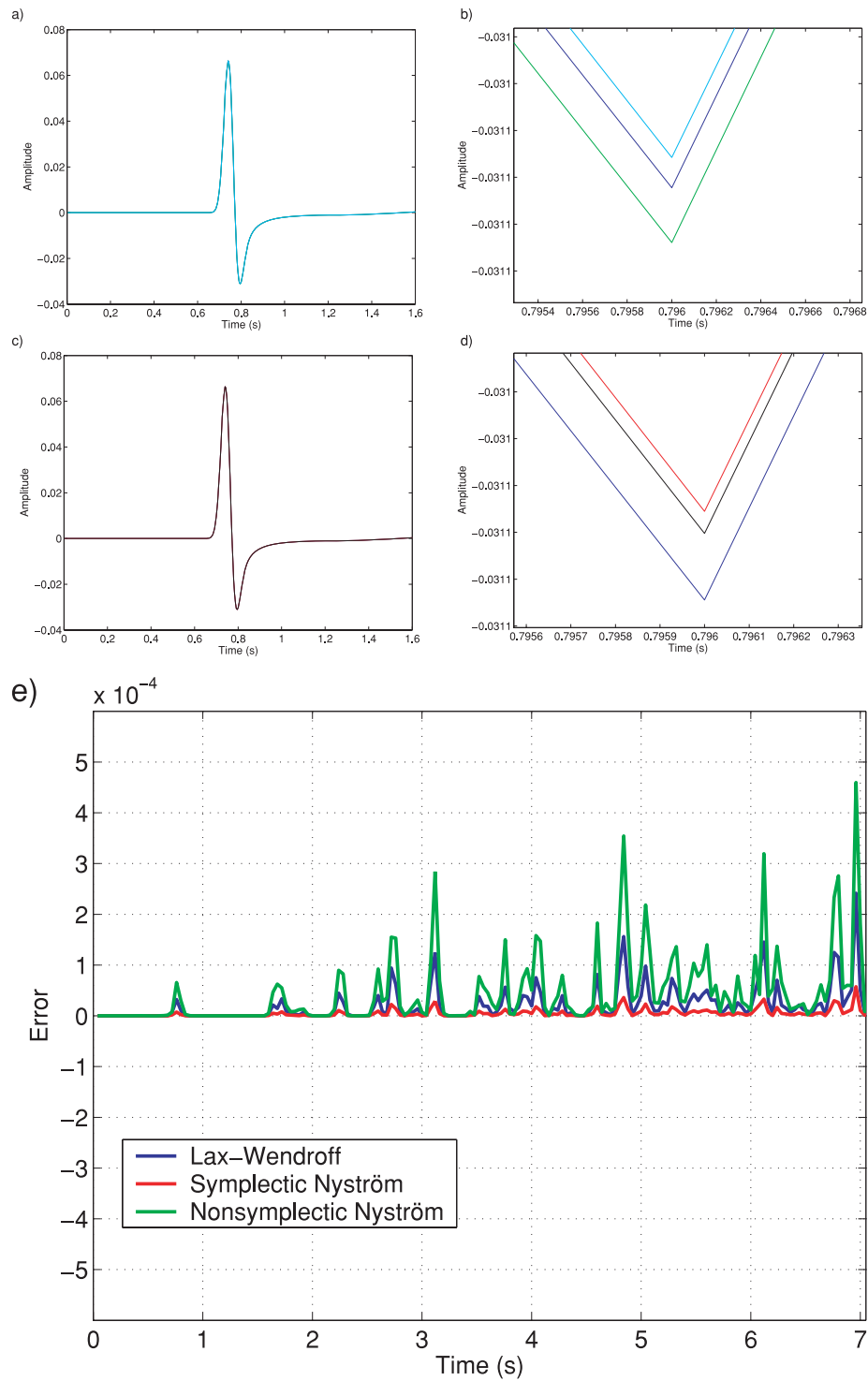


Figure 4 Amplitude curves at a fixed point ($x = -1600$ m, $z = 1600$ m). Plot a: amplitude curves computed with schemes scheme (31) with $\Delta t = 0.004$ s (blue curve), scheme (32) with $\Delta t = 0.004$ s (green curve) and scheme (32) with $\Delta t = 0.002$ s (cyan curve). Plot b: the enlarged portion of plot a. Plot c: amplitude curves computed with scheme (31) with $\Delta t = 0.004$ s (blue curve), scheme (13) with $\Delta t = 0.004$ s (red curve) and scheme (31) with $\Delta t = 0.002$ s (black curve). Plot d: the enlarged portion of plot c. Plot e: the amplitude error computed with schemes (31), (13) and (32).

Here, z_0 is a constant that indicates the position of the source. The grid spacings are $\Delta x = \Delta z = 25$ m. In the following numerical examples, we use periodic boundary conditions.

We consider a Gaussian velocity model (Fig. 3a). This model includes a Gaussian low-velocity area. The wavefields computed with schemes (31), (13) and (32) at $t = 0.92$ s are shown in Figs 3(b), 3(c) and 3(d), respectively. The source is set at ($x = 0$ m, $z = 3200$ m). When the wave travels through the low-velocity area, the slower velocity of the wavefield near the centre causes the incoming wave to focus and form a cusp-shaped front (Fornberg 1987). From these plots, we can see that the three schemes have almost the same performance and they give a qualitatively correct simulation of wave propagation in this medium.

Now we perform a further comparison between the results shown in Fig. 3 but with longer time. To this aim, the amplitude curves at a fixed point ($x = -1600$ m, $z = 1600$ m) will be shown. We first make comparisons between schemes (31) and (32). Figure 4(a) shows the amplitude curves computed with scheme (31) with $\Delta t = 0.004$ s (blue line), scheme (32) with $\Delta t = 0.004$ s (green line) and scheme (32) with a smaller time step size $\Delta t = 0.002$ s (cyan line). In this plot, the three curves are indistinguishable. In the enlarged portion (Fig. 4b), the curves are distinguished and we can see that the blue line is closer to the cyan line than the green line is. Due to its smaller time step size, the cyan line is more accurate than the green line. Therefore, the fact that the blue line is closer to the cyan line indicates that scheme (31) is more accurate than scheme (32). This is because scheme (31) is a second-order symplectic algorithm and scheme (32) is a nonsymplectic algorithm and symplectic algorithms have slower error growth than nonsymplectic ones (Hairer *et al.* 2002). Now using the same method, we make comparisons between schemes (31) and (13). Figures 3(c) and 3(d) (the enlarged portion of Fig. 3c) show the amplitude curves computed with scheme (31) with $\Delta t = 0.004$ s (blue line), scheme (13) with $\Delta t = 0.004$ s (red line) and scheme (31) with a smaller time step size $\Delta t = 0.002$ s (black line). Making the same analysis as above, we can see that scheme (13) is more accurate than scheme (31). This is because scheme (31) is a second-order symplectic algorithm and scheme (13) is a fourth-order symplectic algorithm.

Now we further examine the error growth of the three schemes (31), (13) and (32) with $\Delta t = 0.004$ s. For this purpose, we use the result computed by (13) with a smaller time step size $\Delta t = 0.002$ s as an approximate exact curve. Figure 4(e) shows the absolute value of the amplitude error of the three schemes. We can see that the nonsymplectic scheme (32) has the fastest error growth, the fourth-order symplectic

scheme (13) has the slowest error growth and the second-order symplectic scheme (31) has mediate error growth. This result indicates that the differences in the error growth are determined by the symplecticity and the accuracy of symplecticity of the schemes under consideration although the three schemes both have fourth-order accuracy in temporal discretizations. From this analysis, we can see that the fourth-order Lax-Wendroff scheme is suitable for short-time simulations while the fourth-order Nyström method is suitable for long-time computations.

CONCLUSIONS

I have explored Lax-Wendroff and Nyström methods with spatial pseudospectral discretizations for high-accuracy seismic modelling. The dispersion relation and stability limits of these two kinds of methods are analysed and compared. For practical purposes, one can use the Courant number 0.3 for the fourth-order Lax-Wendroff method to preserve approximately accurate dispersion relation. For eighth-order and higher Lax-Wendroff methods, one can achieve approximately dispersion-free effect at their stability limits. The fourth-order Nyström method has a better dispersion relation but smaller stability limit than the fourth-order Lax-Wendroff method.

The Lax-Wendroff methods are shown to be a second-order symplectic algorithm, regardless of the order of the methods. This result helps us understand the error growth of the Lax-Wendroff methods. Based on the acoustic wave equation, numerical comparisons demonstrate the less error growth of the symplectic methods than nonsymplectic ones. Lax-Wendroff methods are suited for short-term computations, while the Nyström methods are suited for long-term simulations.

ACKNOWLEDGEMENTS

I would like to thank editor Tcheverda and anonymous reviewers for their careful and valuable suggestions, which greatly improved the completeness of this paper. This work was supported by the National Natural Science Foundation of China under grant Nos 40774069 and 40830424.

REFERENCES

- Alford R.M., Kelly K.R. and Boore D.M. 1974. Accuracy of finite-difference modeling of the acoustic wave equation. *Geophysics* **39**, 834–842.

- Blanes S. and Moan P.C. 2002. Practical symplectic partitioned Runge-Kutta and Runge-Kutta-Nyström methods. *Journal of Computational Applied Mathematics* **142**, 313–330.
- Calvo M.P. and Sanz-Serna J.M. 1993. High-order symplectic Runge-Kutta-Nyström methods. *SIAM Journal of Scientific Computing* **14**, 1237–1252.
- Carcione J.M., Herman G.C. and ten Kroode A.P.E. 2002. Seismic modeling. *Geophysics* **67**, 1304–1325.
- Chen J.B. 2006. Modeling the scalar wave equation with Nyström methods. *Geophysics* **71**, T151–T158.
- Chen J.B. 2007. High-order time discretizations in seismic modeling. *Geophysics* **72**, SM151–SM122.
- Dablain M.A. 1986. The application of high-order differencing to the scalar wave equation. *Geophysics* **51**, 54–66.
- Dormy E. and Tarantola A. 1995. Numerical simulation of elastic wave propagation using a finite volume method. *Journal of Geophysical Research* **100**, 2123–2133.
- Fornberg B. 1987. The pseudospectral method: Comparisons with finite differences for the elastic wave equation. *Geophysics* **52**, 483–501.
- Fornberg B. 1996. *A Practical Guide to Pseudospectral Method*. Cambridge University Press.
- Gazdag J. 1981. Modeling of the acoustic wave equation with transform methods. *Geophysics* **46**, 854–859.
- Hairer E., Lubich C. and Wanner G. 2002. *Geometric Numerical Integration: Structure-preserving Algorithms for Ordinary Differential Equations*. Springer-Verlag.
- Hairer E., Nøsett S.P. and Wanner G. 1993. *Solving Ordinary Differential Equations I*. Springer-Verlag.
- Kelly K.R., Ward R.W., Treitel S. and Alford R.M. 1976. Synthetic seismograms: A finite-difference approach. *Geophysics* **41**, 2–27.
- Komatitsch D. and Vilotte J.P. 1998. The spectral element method: An efficient tool to simulate the seismic response of 2D and 3D geological structures. *Bull. Seism. Soc. Am.* **88**, 369–392.
- Kosloff D. and Baysal E. 1982. Forward modeling by the Fourier method. *Geophysics* **47**, 1402–1412.
- Kosloff D., Reshef M. and Loewenthal D. 1984. Elastic wave calculations by the Fourier method. *Bulletin of the Seismological Society of America* **74**, 875–891.
- Lunk C. and Simen B. 2005. Runge-Kutta-Nyström methods with maximized stability domain in structural dynamics. *Applied Numerical Mathematics* **53**, 373–389.
- Marfurt K.J. 1984. Accuracy of finite-difference and finite-element modeling of the scalar and elastic wave equations. *Geophysics* **49**, 533–549.
- Nyström E.J. 1925. Über die numerische Integration von Differentialgleichungen. *Act. Soc. Sci. Fenn.* **50**, 1–54.
- Okunbor P.J. and Skeel R.D. 1992. Canonical Runge-Kutta-Nyström methods of orders 5 and 6; Working Document 92-1, Dep. Computer Science, University of Illinois.
- Qin M.Z. and Zhu W.J. 1991. Canonical Runge-Kutta-Nyström methods for second order ODE's. *Computational Mathematics Applications* **22**, 85–95.
- Sanz-Serna J.M. and Calvo M. 1994. *Numerical Hamiltonian Problems*. Chapman and Hall, London.
- Tal-Ezer H., Kosloff D. and Koren Z. 1987. An accurate scheme for seismic forward modeling. *Geophysical Prospecting* **35**, 479–490.
- Tsitouras Ch. 1999. A tenth-order symplectic Runge-Kutta-Nyström method. *Celestial Mechanics of Dynamic Astronomy* **74**, 223–230.
- Virieux J.E. 1986. P-SV wave propagation in heterogeneous media: Velocity-stress finite-difference method. *Geophysics* **51**, 888–901.